Dislocation-mediated growth of bacterial cell walls

Ariel Amir and David R. Nelson[1]

Department of Physics, Harvard University, Cambridge, MA 02138

Recent experiments have illuminated a remarkable growth mechanism of rod-shaped bacteria: proteins associated with cell wall extension move at constant velocity in circles oriented approximately along the cell circumference [Garner EC, et al., (2011) *Science* 333:222–225], [Domínguez-Escobar J, et al. (2011) *Science* 333:225–228], [van Teeffelen S, et al. (2011) PNAS 108:15822–15827]. We view these as dislocations in the partially ordered peptidoglycan structure, activated by glycan strand extension machinery, and study theoretically the dynamics of these interacting defects on the surface of a cylinder. Generation and motion of these interacting defects lead to surprising effects arising from the cylindrical geometry, with important implications for growth. We also discuss how long range elastic interactions and turgor pressure affect the dynamics of the fraction of actively moving dislocations in the bacterial cell wall.

biophysics | cell wall growth | microbiology

Bacterial cell walls are composed of peptidoglycan (also called murein), which endows them with shape and rigidity. The architecture and growth of cell walls have been the subject of active research for many decades, in particular for gram-negative bacteria whose cell walls consist of single or few layers of glycan strands crosslinked by peptides (1–4). While some models assume a very ordered structure, recent experimental work (5) suggests the structure is more disordered. We view the peptidoglycan mesh as a partially ordered two-dimensional crystal with a large number of defects to account for the disorder in the structure. The rod shape of many bacteria (e.g., *Escherichia coli*), together with mutant variants that grow but fail to complete cell division, make a cylindrical geometry a natural one to study. To easily add material to this ordered structure, one must clearly break the periodicity and create a defect in the structure. An especially important class of defects are termed dislocations, known to be important in determining the mechanical properties of metals and other crystalline or polycrystalline materials, such as their strength and plasticity (6). Dislocations are known to have long-ranged elastic interactions, which are logarithmic in the distance (but not isotropic, as is the case for vortices in superfluids). The "elementary charge" of these topological defects is the Burgers vector $\vec{b}$, which is often at right angles to the direction of insertion of the new strand of material, and is a lattice vector of the structure. Here, we apply dislocation theory to the problem of bacterial growth, proposing a simplified model inspired by the elongation of bacterial cell walls, which we are able to solve both analytically and via computer simulations. Fig. 1 illustrates an idealized picture of defects in a cylindrical geometry. For simplicity, we show a square lattice with lattice vectors parallel and perpendicular to the cylinder's long axis, although the actual peptidoglycan mesh is rectangular [and in fact the lattice vectors might have a nontrivial angle with respect to the cylinder's axis (7)].

The model treated below will in fact consist of a *large* number of dislocations, and so the structure we treat is far from a perfect crystal. Working with defects of a crystal provides a convenient and numerically efficient method to take the disorder into account. We expect that the unit cell of Fig. 1 typically contains two glycan strands, as it is only this larger unit cell that respects the local crystalline symmetry; see for example refs. 8, 9. Recent experiments on both gram-negative (10) and gram-positive bacteria

(11, 12) track fluorescently labeled proteins such as MreB known to correlate strongly with the addition of peptidoglycan subunits, and have shown that these proteins move at roughly constant velocity, approximately along the cylinder's circumference. We view these strand extension centers as edge dislocations in the ordered structure, with a Burgers vector oriented along the cylinder's long axis (the direction of the Burgers vector depends on the direction of insertion of the new strand, see Fig. 1). Extending the end of an inserted strand (i.e., the core of an edge dislocation) involves breaking peptide bonds to allow extra sugar units into the lattice, together with additional short peptide cross-links (1). In dislocation theory, this type of motion is referred to as dislocation *climb*. In the following, we treat the protein motion and the dislocation motion synonymously, assuming that the motion of the MreB and its associated enzymes is fully correlated with the insertion of new material into the cell wall. This idea was introduced in ref. 9, and here we develop it further and deduce various biological insights and predictions. As pointed out by Burman and Park (13), glycan strand extension is somewhat analogous to the action of a DNA polymerase. Our dislocation perspective allows us to take into account long-range elastic interactions between the "murein extension centers" of ref. 13.

Although extensive work has been done on dislocation theory over the last century (6), this biophysics problem is quite different from materials science and condensed matter physics in several respects: the climb of dislocations necessarily involves the exchange of material, which in 3D crystals involves diffusion of interstitials or vacancies. Hence, except at high temperatures, dislocation glide dominates the dynamics. [Because the bacterial cell walls are characterized by strong (peptide and glycan) bonds (1), neither glide nor climb would be possible in this case without the aid of the strand extension proteins at physiological temperatures.] Here, dislocation climb is the central process mediating cell wall growth, with sugars and amino acids essential for the climb process synthesized and arriving from the interior of the bacterium. A second, obvious, difference, regards the unusual cylindrical geometry which we study here. This feature leads to a number of interesting properties, such as the exponential decay of dislocation interactions along the cylinder's long axis, as discussed below. Dislocations in a cylindrical geometry were considered in a very different biophysics problem in ref. 14, studying tail-sheath contraction in a bacteriophage. A final difference from conventional materials science is that here the dislocation climb itself alters the geometry, as it is this very motion that grows the cell wall along the axis of the cylinder. This idea can be used to estimate the number of actively climbing dislocations per bacterium, using experimental data: The typical time of division of the bacteria is of the order of tens of minutes, in which the bacteria elongate by approximately 1 μm. The lattice spacing of the peptidoglycan along the long axis, b, is believed to be of the order of several nanometers (1). If we assume the area of the hemisphe-
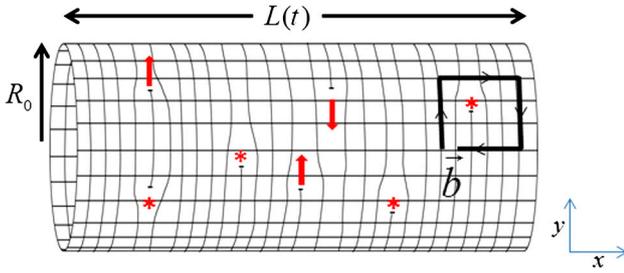
Fig. 1. Schematic illustration of active (arrows) and inactive (asterisk) dislocations in an otherwise ordered peptidoglycan mesh. The dislocations with arrows attached are activated by the enzymatic machinery and move with velocity *v*. Those with asterisks are inactive.

rical end caps remains fixed, the dynamics of the cylindrical surface area $S(t)$ (taking all dislocations as completely independent, for now), is given by:

$$\frac{dS}{dt} = N_{ac} v b, \qquad [1]$$

where N_{ac} is the total number of actively moving dislocations and v is their velocity. Taking the measured velocity v to be several tens of nanometers/second (10–12), we find that *a few tens* of active dislocations moving along the circumference and growing the cell wall would be sufficient to account for the measured growth rate. This estimate is consistent with pioneering work of ref. 13, obtained using a very different method of radioactive labeling. Current technology does not yet enable a direct determination of N_{ac}, because only a subset of the total number of active dislocations is fluorescently marked (10–12).

The structure of the manuscript is as follows. We first define the model and the approximations made, and describe the force on a dislocation, including the elastic interactions between dislocations on a cylinder. The implications of the large turgor pressure inside the bacterium and the effects of the long-ranged elastic interactions are highlighted. We then propose a set of equations for the growth dynamics and its coupling to the numbers of active and inactive dislocations, and show that they often lead to exponential lengthening of a single bacterium. The exponential growth rate itself depends on a few simple parameters, with a well defined microscopic interpretation. The theoretical expectations are illustrated and visualized by numerical simulations, both in the main text and *SI Text*. A numerical calculation presented in *SI Text* is used to estimate the disorder strength due to the elastic interactions with a large number of randomly positioned dislocations, chosen according to the biological parameters. Certain parameters of the rate-equations model [Eqs. **5** and **6**], can not be determined from a numerical simulations, and are dictated by the underlying biochemistry, for example $v(G)$ (the dependence of the dislocation velocity on the driving force) and the dislocation processivity γ_1.

The Model

Interesting recent works have modeled and simulated the peptidoglycan structure in molecular detail, and have predicted a number of nontrivial phenomena which were indeed observed experimentally (15, 16). Our approach is somewhat different (and perhaps complementary), because we study a highly simplified model and focus on a relatively dilute concentration of defects (both actively moving and frozen) in an otherwise regular peptidoglycan mesh. As a result both analytic and numerical progress is possible, although we suppress fine details of the structure.

Consider, motivated by bacterial cell wall growth, a number of interacting edge dislocations with a Burgers vector $\vec{b}$ oriented in both directions along the cylinder's long axis, as illustrated schematically in Fig. 1. The radius of the cylinder, R, will be assumed

to be constant, as is approximately true for rod-shaped bacteria. For simplicity, consider an infinite cylinder, neglecting the effects of the boundaries [Experiments indicate that strand extension dynamics does not change significantly near the cylinder's end caps, consistent with this assumption (11).].

We also simplify by assuming linear elasticity, except near dislocation cores. Various works have indicated, both from the theoretical (17) and experimental (18) perspective, that the high osmotic pressure (18, 19), referred to as turgor pressure in bacteria and plant cells, produces large strains compared to the relaxed state. We shall take the elastic moduli as constants, which in practice should be considered as effective constants relative to the working turgor pressure.

In order for a dislocation to be able to "climb" [i.e., move perpendicular to its Burgers vector (6) and contribute to the growth process], various proteins have to be present at the dislocation core, responsible for "recruiting" and assembling the sugars and peptides necessary for the construction of the peptidoglycan mesh. Hence, we separate the dislocations into two populations, active and inactive ones. Inactive defects still exert elastic forces on the active ones, and create an effective disordered energy landscape for them. The cores of inactive dislocations also represent favorable locations for the creation of new active dislocations: the elongation machinery can attach to the free strands (i.e., the inactive dislocations), creating active ones. The finite processivity of the elongation machinery will also give rise to the opposite process, whereby an active dislocation can become inactive when the machinery falls off. In general, the rates of these processes will not balance, because the system is never in steady-state but is instead constantly growing via dislocation climb, as it incorporates material from the third dimensions, a situation rarely encountered in conventional materials science (6).

The Force on a Dislocation. Elastic stresses exert a Peach-Koehler force (6, 20) on a dislocation [analogous to the Magnus force acting on vortices (21)] which in our case is given by:

$$F_x = b\sigma_{xy}; \qquad F_y = -b\sigma_{xx}, \qquad [2]$$

where σ is the 2D stress tensor of the peptidoglycan mesh, and we assume a Burgers vector along the *x*-axis.

For a cylinder of radius R we have $\sigma_{yy} = 2\sigma_{xx} = pR$, where x denotes the coordinate along the long axis, and p is the turgor pressure, and $F_y = -\frac{1}{2} bpR$. In addition to the contribution of the turgor pressure, if the free energy is changed by U by the biochemical process of adding one unit cell to the peptidglycan mesh, it will contribute an additional force of U/b in the y direction, as can be seen using the principle of virtual work.

Under physiological conditions, we expect that the dislocations are in the overdamped regime, with the dislocation velocity proportional to the force, i.e., $v_i = \sum_j \mu_{ij} F_j$, where μ_{ij} is a mobility tensor with glide and climb components that depends on the extension machinery and the abundance of sugars, peptides, etc. In the following we assume that μ_{ij} is diagonal, with μ_{xx} and μ_{yy} describing glide and climb mobilities, respectively. We expect that the mobility tensor itself will have a turgor pressure dependence, as the resulting forces can lower the activation barriers of the various biochemical pathways involved in the process. Thus, the observed velocity of the strand extension machinery should depend on the excess pressure for rod-shaped bacteria.

The Role of Interactions. In condensed matter physics, the long-range elastic interactions between dislocations can have important consequences, and have recently been suggested to lead to glassy effects and nonthermal, heavy-tailed, dislocation velocity distributions (22–24).

To illuminate the importance of interactions in a biological context, we have solved for the interaction energy of two disloca-

tions with antiparallel Burgers vectors $\pm\vec{b}$ on an infinite cylinder, separated by a distance x along the long-axis and y along the circumference: [For the detailed derivation, see *SI Text*].

$$E(x,y) = \frac{Ab^2 h}{2}\left[i\frac{x}{2R}\csc\left(\frac{y}{2R}\right)\sinh\left(\frac{x}{2R}\right)\mathrm{csch}\left[\frac{x-iy}{2R}\right]\right.$$
$$\left. + \log\left(\frac{2R}{b}\sinh\left[\frac{x-iy}{2R}\right]\right)\right] + \text{C.C.} \qquad [3]$$

Here, R the radius of the cylinder, h the cell wall thickness, and $A \equiv \frac{\mu}{2\pi(1-\nu)}$, with μ the shear modulus and ν the Poisson ratio (we assume isotropic elasticity theory, for simplicity). For distances $x \gg R$ along the axis of symmetry, Eq. 3 shows that the interactions fall off exponentially. For distances much smaller than the cylinder radius, the interaction energy reduces to its form in two-dimensions, as expected. Clearly, the relevant scale for the interaction energy is $Ab^2 h$. Fig. S1*A* shows an example of the equal energy contours. Close to the origin, taking a cut parallel to the x-axis would give a graph with two minima, corresponding to the two dislocations sitting at a 45° angle—this is expected, because the physics close to the origin should be insensitive to the finite cylinder radius: this arrangement is indeed the stable configuration of two dislocations in Euclidean space, when climb processes are prohibited (25). Fig. S1*B* illustrates how interactions affect an activated dislocation (i.e., one with strand-extending machinery attached) attempting to move upwards from a fixed, unactivated defect. See also Fig. S2 illustrating the effects of strong interactions on the dislocation dynamics.

Let G represent the combined effect of the chemical forces provided by enzyme-mediated polymerization and those caused by turgor pressure, as described by Eq. 2. The sign of this force depends on the sign of the Burgers vector, and acts in the direction which corresponds to elongation of the existing strands. For a vertical separation y in the range $b < y \ll 2\pi R$, we can use Eq. 3 and add a term $E_{\mathrm{field}} = -Gy$ corresponding to the force G. The total potential energy is $U(y) = 2E_c + (Ab^2 h)\log(y/b) - Gy$, where $2E_c$ is the energy at separation $y = b$ and $G = 0$. The logarithmic interaction term clearly leads to a long-range elastic force that falls off slowly, like $1/y$. Upward motion will require thermal activation unless $y > y^* = Ab^2 h/G$. Escape from this logarithmic binding will be relatively easy for G large enough to insure $y^* \leq b$, i.e., $G > G^* \equiv Abh$. Healthy, growing cells in rich nutrient environments are likely to be in this regime and thus escape the confining effect of elastic forces. Elastic interactions will nevertheless become important when G is diminished by osmotic shock, nutrient deprivation, or by application of antibiotics that interfere with the powerful strand extension machinery.

Fig. 2 illustrates the dynamics of several tens of active dislocations under the influence of a circumferential "field" or driving force G on each dislocation with pairwise elastic interactions given by Eq. 3, moving in the disordered background created by inactive dislocations, to be elaborated upon below. For a weakly disordered system, one obtains ordered circumferential motion (see Fig. S3), while for a disorder level chosen according to the biological parameters, the elastic interactions are strong enough to occasionally pin the motion. These pinning events could be related to pauses in the circumferential motion observed in recent experiments (11). The condition for pinning to be important follows from comparing the typical elastic interaction force with the nearest dislocation a distance r_{nn} away (which is highly likely to be inactive) and the net driving force G. Pinning is expected to occur when:

$$\frac{Ahb^2}{r_{nn}} = Ahb^2 n^{1/2} > G,$$

where n is the dislocation areal density. With parameter estimates for *E. coli* (see *SI Text*) we find that the ratio $\chi \equiv Ahb^2 n^{1/2}/G$ is of the order of unity, suggesting that pinning events are likely to
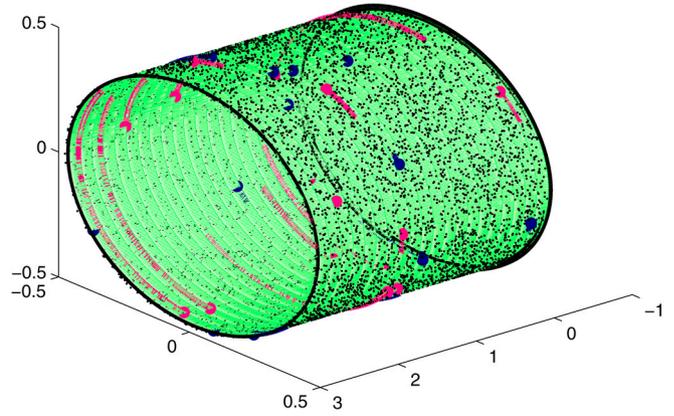

Fig. 2. Numerical simulation of the dynamics of 30 active dislocations, with simulation parameters matching the biological ones. The dislocations are driven by a combination of chemical forces and turgor pressure in the circumferential direction, proportional to the sign of the Burgers vector. 10,000 inactive dislocations create a disordered potential for the motion of the active dislocations. The temperature is zero and $\frac{2\pi RG}{Ab^2 h} = 450$. The x and y coordinates of the dislocations were chosen randomly and uniformly along the axes, and $W/L = \frac{2\pi R}{L} = 1$. The climb to glide mobility ratio is $\mu_c/\mu_g = 10$. The red and blue points mark the starting positions of the $\pm b$ dislocations, and the red and blue lines correspond to their trajectories. The black circles mark the end of the cylinder. A snapshot of the simulation is taken after $t = 0.7\frac{W}{\mu_c G}$. The numerous inactive dislocation (marked as black dots) create a disordered energy landscape which can trap the active dislocations and inhibit further growth. *In the SI Text further details regarding the simulation are given, as well as Movie S1 showing the dynamics.*

occur. However, due to the finite processivity of the active dislocations, pinning can be bypassed by the growth dynamics, as the elongation machinery can drop off a pinned dislocation and continue the strand elongation elsewhere. However for biological conditions (nutrient depletion or low turgor pressure) such that $\chi \gg 1$, pinning events could become much more important.

Evidently, experimental measurements of interaction-induced correlations between moving dislocations could provide a useful probe of the elastic properties of the peptidoglcan. Estimates of the relative strength of the interactions compared to the other forces involved in the problem are provided in *SI Text*, and discussed below.

Dislocation Dynamics

Eq. 1 expresses the rate of change of the bacterial surface area $S(t)$. To proceed further, we must account for the dynamics of the number of active and inactive dislocations, controlled by a variety of interesting biological processes:

1. Dislocation pair creation: it is plausible that the nucleation of new growth sites should be proportional to the cylinder's area (see Fig. 3*B*). For growth under rich nutrient conditions, we expect the area *density* of peptidoglycan growth sites (i.e., activated dislocations) to be constant, which requires a source of new dislocations as the bacterium elongates with fixed radius. Dislocation pairs could in principle be created by thermal activation* (25), although this process is likely to be rare in a covalently bonded peptidoglycan mesh. Alternatively, a dislocation pair can form by breaking bonds in the peptidoglycan mesh, via an enzymatic process or via external damage by radiation or severe stresses. If the G force is small, dislocation pairs will remain tightly bound and not contribute to the growth process. Henceforth, our discussion of the bacterial elongation will assume that $G \gtrsim G^*$, the critical unbinding force discussed previously, although it is not difficult to relax this assumption.

---

*Amir A, Nelson DR, *Topological defects in cylindrical geometries*.

2. The finite processivity of elongation enzymes: the elongation machinery can fall off an active dislocation, and render it inactive. In an elegant recent work (26), finite processivity was implicated in straightening of an initially curved *Caulobacter crescentus*, where the working hypothesis was that the growth occurs via partial "hoops" extending perpendicular to the long axis of the rod-shaped bacteria, as described in refs. 10–12. For *C. crescentus*, processivity was such that on average 1/5 of the circumference is traversed before the machinery falls off (26). It would be interesting to perform a similar study for *E. coli* or *Bacillus subtilis*. Growing filamentous *E. coli* in curved microchambers was also demonstrated (27), proving the feasibility of such an experiment for *E. coli*.

3. The activation of an inactive dislocation: the reverse process assembles the elongation machinery onto an existing (static) glycan strand end and turns it into an actively growing dislocation. The rate of this process is proportional to the number of inactive dislocations.

4. Annihilation processes: two dislocations, both active or one inactive, can "collide", completing a full circumferential strand. The elongation machinery could then immediately continue to move and grow the cell wall (as in Fig. 3A), in which case the annihilation process plays no role. Alternatively, the elongation machinery could tie the strands together, dislodge and become available for a new inactive dislocation. In complete analogy to the theory of chemical reactions, the rate of this latter process per unit area is proportional to the product of the density of the active dislocation and that of the total number of dislocations.

Upon collecting together these four processes, we describe the dynamics of the numbers of active and inactive dislocations on a cylindrical wall of surface area $S(t)$ by supplementing Eq. **1** with the following:

$$\frac{dN_{ac}}{dt} = \Gamma S - \gamma_1 N_{ac} + \gamma_2 N_{in} - \gamma_3 v N_{ac}(n_{ac} + n_{in}), \qquad [5]$$

$$\frac{dN_{in}}{dt} = \Gamma S + \gamma_1 N_{ac} - \gamma_2 N_{in} + 2\gamma_4 S - \gamma_3 v n_{ac} N_{in}. \qquad [6]$$

In the above, N_{ac} and N_{in} denote the number of active and inactive dislocations, and $n_{ac} = N_{ac}/S$ and $n_{in} = N_{in}/S$ denote their densities. The term Γ arises from the nucleation of dislocation pairs, one active and one inactive, by a process like that shown in Fig. 3B, while γ_1 represents the processivity and γ_2 describes the activation of an inactive dislocation (see Fig. 3A). The
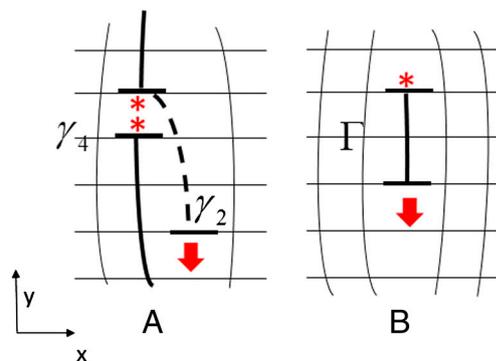

Fig. 3. (*A*) Active dislocation pulled past an inactive one by the enzymatic machinery. In this case an initial (inactive) dislocation pair could be created by an enzyme that cuts glycan bonds (rate constant γ_4). The elongation machinery then assembles around an inactive dislocation turning it into an active one (rate constant γ_2). (*B*) Direct insertion of a glycan strand fragment to create an active and inactive dislocation pair (rate constant Γ).

rate γ_3 represents the annihilation of a dislocation pair (which is typically proportional to the velocity). Finally, γ_4 describes creation of tightly bound inactive dislocation pairs by an enzyme which adds to the reservoir of activatable dislocations by cutting covalent bonds (Fig. 3A). Note that no spatial structure is present in the above equations: the dynamics is "mean-field" like; i.e., it assumes that the dislocations are well mixed and that their density is approximately uniform on the cylinder. A more sophisticated theory would explore the effects of spatial heterogeneities on the dynamics. In ref. 9, a simplified dynamical description in terms of an active dislocation density limited by a pair-annihilation cross-section was proposed. The more general approach taken here includes inactive dislocations explicitly, and incorporates the geometrical dilution phenomenon discussed below.

We search for steady-state densities n_{ac} and n_{in} with these equations, taking into account Eq. **1**. The steady-state dislocation densities then obey:

$$n_{ac}^2 vb = \Gamma - \gamma_1 n_{ac} + \gamma_2 n_{in} - \gamma_3 v n_{ac}(n_{ac} + n_{in}), \qquad [7]$$

$$n_{in} n_{ac} vb = \Gamma + \gamma_1 n_{ac} - \gamma_2 n_{in} + 2\gamma_4 - \gamma_3 v n_{ac} n_{in}. \qquad [8]$$

The terms on the left arises because the dislocations are automatically diluted as the cell wall grows. From Eq. **1**, we see that the length of the bacterium $L(t) = \frac{S(t)}{2\pi R}$ grows exponentially in the steady state,

$$L(t) = L_0 e^{n_{ac} vbt}. \qquad [9]$$

While we cannot rule out the possibility of cell cycle effects in the elongation rate, our simplified model is consistent with the existing data for exponential growth, for bacteria growing in one dimensional channels with abundant nutrients (28). As discussed below, the G force driving dislocation climb enters our dynamical equations, through (1) $\Gamma(G)$, the escape rate of bound dislocations, (2) the velocity $v = v(G)$, (3) through the capture cross-section embodied in $\gamma_3 = \gamma_3(G)$, and (4) the creation rate of new dislocations. In particular Γ and γ_4 might depend on G, as it could change the barriers for thermal activation (see ref. 29 for a related discussion).

The Biological Parameters

In *SI Text*, we estimate the relevant biological parameters for the case of *E. coli*, in order to elucidate which of the previous physical processes should be important. We estimate the energy of creating a new dislocation pair using the measured elastic constants, and find that it is much larger than the temperature. Using the measured turgor pressure, we find that the force exerted on each of the dislocation by the stresses arising from it is similar in strength to those due to the biochemical reaction involved in the elongation process. This estimate suggests that changing the turgor pressure or alternatively, putting the bacteria under mechanical stresses, can result in significant changes in the velocity of the dislocations. The density of *inactive* dislocations can be estimated from the strand length distribution, and is found to be much larger than that of *active* dislocations. Finally, the typical elastic interaction forces between nearby *active* dislocations are negligible compared to the driving force in the circumferential direction, but the elastic interactions between the *active* dislocations and the numerous *inactive* ones are comparable to the driving force, suggesting that the possibility of dislocation pinning, discussed earlier, could occur.

Bacterial Elongation Rate

The assumption $n_{in} \gg n_{ac}$ simplifies Eqs. **5** and **6**. We explore here two possible scenarios:

1. *A two-stage process:* An enzyme cuts glycan links in the mesh to produce a pair of inactive dislocations, while other proteins possibly recruited by the MreB then activate a small subset of them, accounting for the small subset of active dislocations (see Fig. 3*A*). Thus far, the annihilation of dislocations does not seem to be observed in experiments, suggesting that we could also ignore γ_3. With these assumptions, we can simplify Eqs. **5** and **6** in the steady state: $n_{ac}^2 vb = \gamma_2 n_{in} - \gamma_1 n_{ac}$, $n_{in} n_{ac} vb = \gamma_1 n_{ac} - \gamma_2 n_{in} + 2\gamma_4$.

Upon adding these equations and using $n_{in} \gg n_{ac}$ we obtain: $n_{in} n_{ac} vb = 2\gamma_4$, which when combined with the previous equations leads to a cubic equation for n_{ac}, the density of active dislocations:

$$n_{ac}^3 b^2 v^2 + \gamma_1 n_{ac}^2 bv = 2\gamma_2 \gamma_4. \qquad [10]$$

For $bv\gamma_2\gamma_4 \gg \gamma_1^3$ (short processivity of the elongation machinery) we find $n_{ac} = \left(\frac{2\gamma_2\gamma_4}{b^2 v^2}\right)^{\frac{1}{3}}$, while for $bv\gamma_2\gamma_4 \ll \gamma_1^3$ we get $n_{ac} = \sqrt{\frac{2\gamma_2\gamma_4}{bv\gamma_1}}$.

It is useful to rewrite these scaling relations in terms of the exponential growth rate $\lambda = n_{ac}vb$, where $L(t) = L_0 e^{\lambda t}$. One obtains the relations: $\lambda = (2bv\gamma_2\gamma_4)^{\frac{1}{3}}$, for short processivity, and: $\lambda = \sqrt{\frac{2bv\gamma_2\gamma_4}{\gamma_1}}$ in the opposite regime. An experimentally accessible control (e.g.: temperature) for which one of the microscopic processes (e.g.: γ_1) is much more sensitive than the others, would provide a way to test these scaling relations without experimentally measuring *all* of the microscopic rates.

2. *Direct insertion of a nascent strand:* Another possible scenario is that dislocation pairs are formed by inserting material into the mesh (but on new sites, between the existing mesh, see Fig. 3*B*), which are further acted upon by the elongation machinery to produce the growth. If this direct insertion is the dominant mechanism we can neglect γ_4. If in addition we neglect the annihilation term, as discussed previously, we obtain the steady-state equations: $n_{ac}^2 vb = \Gamma - \gamma_1 n_{ac} + \gamma_2 n_{in}$, $n_{in} n_{ac} vb = \Gamma + \gamma_1 n_{ac} - \gamma_2 n_{in}$.

Upon again invoking $\frac{n_{in}}{n_{ac}} \gg 1$, we find that $n_{ac} n_{in} bv \approx 2\Gamma$, which leads to a quadratic equation for n_{ac}:

$$\gamma_1 n_{ac}^2 - \Gamma n_{ac} - \frac{2\gamma_2 \Gamma}{bv} = 0. \qquad [11]$$

For $\gamma_1 \gg \frac{\Gamma bv}{\gamma_2}$, we obtain $n_{ac} \approx \sqrt{\frac{2\gamma_2\Gamma}{\gamma_1 bv}}$.

Another useful limit can be obtained by setting $\gamma_2 = 0$. In this limit active dislocations can only be created by the direct insertion, and inactive dislocations to not play a role. In this case, which was studied in ref. 9, the two equations decouple, and one obtains a quadratic equation for n_{ac}.

We anticipate that experiments will soon determine the density of active dislocations, thus allowing tests of the above scaling relations. As explained previously, parameters such as the processivity could be experimentally determined independently, allowing additional checks. Another interesting biological scenario is one where the creation of new dislocations is abruptly stopped, by disabling the relevant protein. In this case $\gamma_4 = \Gamma = 0$, and subsequent steady-state growth is *linear* rather than exponential, because the total number of dislocations is constant in this case. From Eqs. **5** and **6** we can determine the typical transient time τ for the growth to cross over to the linear regime is, $\tau = \frac{1}{\gamma_1 + \gamma_2}$. This and related experiments could provide further insight into the microscopic rate constants discussed above.

Protein regulation and exponential growth. Cell wall growth by itself is unlikely to be a bottleneck process that limits bacterial growth (30). In fact, bacterial cells probably regulate the concentration of all proteins, DNAs, RNAs, *etc.* involved in the cell growth, to yield a coordinated set of doubling times determined by richness of the media, temperature, *etc.* In our model, parameters such as the dislocation velocity, driving force G, and density of active dislocations will be determined by the regulatory network that controls cell growth. One important feedback mechanism is surely "geometrical dilution": as the cell wall grows, the concentrations of all the proteins in the cells are diminished. If we assume ribosome production is the limiting factor of the growth (31) (ribosomes constitute of most of the dry weight of the cell), and the relevant proteins are maintained at constant *concentration*, the cell wall dynamics discussed here would be consistent with the ribosomal constraints. Regulation of concentration is appealing, as it is a local and robust mechanism, consistent with the biological ideas about self-organization (32). Locality is also connected with the appearance of the surface area in Eqs. **5** and **6**, as discussed earlier. Even if some more complicated biological process is involved, we expect predictions such as Eqs. **7** and **8** to hold; one should be able to check them directly by measuring the rates of the underlying individual processes, and by engineering sudden changes in rates such as γ_1, γ_2, or γ_4. Finally, we note that the aforementioned geometric dilution is quite generic, and will appear in every case where the cell volume grows. In ref. 33, section 2.4, this dilution is accounted for by adding a term to the protein degradation rate. In our case, however, the dilution of the *active* dislocations is not proportional to their concentration (as is usually the case with protein degradation), but enters *quadratically*. The quadratic dependence arises since the active dislocations themselves are responsible for the change in surface area.

Conclusions and Outlook

In this paper we used the continuum elastic theory to account for recent experiments on the growth of a single bacterium. Our theoretical framework exploits the partially ordered structure of the peptidoglycan mesh to obtain an economical description of the growth dynamics in terms of dislocation defects. The forces acting on these defects lead to predominantly *climb* dynamics, quite different from those typically found in condensed matter physics and materials science. Our results suggest that osmotic pressure could affect the measured dislocation velocities, and that the elastic interactions could lead to pinning of the dislocation motion. Consideration of various processes associated with dislocation motion, and their creation and annihilation, leads to a coupled set of ordinary differential equations that govern the dynamics of the number of active and inactive dislocations, and the overall elongation rate. Solving these under conditions of abundant nutrients leads to exponential growth, consistent with the experimental observations. Transients and other modes of growth are also discussed. In the future, it would be interesting to compare and contrast bacterial elongation with pollen tube growth, another case where the growth occurs on a cylinder with an approximately constant radius (34). One might also speculate that planar arrangements of cells in, say, embryos, grow by cell divisions sited preferentially in dislocation cores. The resulting dislocation climb takes place in an array of living cells, as opposed to the much smaller *unit cells* in a peptidoglycan mesh. Another natural extension of this approach might be to model the growth of approximately spherical cells (9), such mutant *E. coli*. Finally, it would be useful to extend this theory to the thicker cell walls of gram-positive bacteria, which experimentally show similar phenomenology (11, 12).

1. Young KD (2010) Bacterial shape: two-dimensional questions and possibilities. *Annu Rev Microbiol* 64:223–240.
2. Sun SX, Jiang H (2011) Physics of bacterial morphogenesis. *Microbiol Mol Biol R* 75:543–565.
3. Scheffers DJ, Pinho MG (2005) Bacterial cell wall synthesis: new insights from localization studies. *Microbiol Mol Biol R* 69:585–607.
4. Vollmer W, Blanot D, De Pedro MA (2008) Peptidoglycan structure and architecture. *FEMS Microbiol Rev* 32:149–167.
5. Gan L, Chen S, Jensen GJ (2008) Molecular organization of gram-negative peptidoglycan. *Proc Natl Acad Sci USA* 105:18953–18957.
6. Hirth JP, Lothe J (1982) *Theory of Dislocations* (Wiley, New York).
7. Wang S, Furchtgott L, Huang KC, Shaevitz JW (2012) Helical insertion of peptidoglycan produces chiral ordering of the bacterial cell wall. *Proc Natl Acad Sci USA* 109:E595–E604.
8. Vollmer W, Bertsche U (2008) Murein (peptidoglycan) structure, architecture and biosynthesis in *Escherichia coli*. *Biochim Biophys Acta* 1778:1714–1734.
9. Nelson D. R. (2012) Biophysical dynamics in disorderly environments. *Ann Rev Biophysics* 41:371–402.
10. van Teeffelen S, et al. (2011) The bacterial actin mreb rotates, and rotation depends on cell-wall assembly. *Proc Natl Acad Sci USA* 108:15822–15827.
11. Garner EC, et al. (2011) Coupled, circumferential motions of the cell wall synthesis machinery and mreb filaments in B. subtilis. *Science* 333:222–225.
12. Domnguez-Escobar J, et al. (2011) Processive movement of mreb-associated cell wall biosynthetic complexes in bacteria. *Science* 333:225–228.
13. Burman LG, Park JT (1984) Molecular model for elongation of the murein sacculus of *Escherichia coli*. *Proc Natl Acad Sci USA* 81:1844–1848.
14. Olson GB, Hartman H (1982) Martensite and life: displacive transformations as biological processes. *Journal de Physique* 43:C4–855.
15. Huang KC, Mukhopadhyay R, Wen B, Gitai Z, Wingreen NS (2008) Cell shape and cell-wall organization in gram-negative bacteria. *Proc Natl Acad Sci USA* 105:19282–19287.
16. Furchtgott L, Wingreen NS, Huang KC (2011) Mechanisms for maintaining cell shape in rod-shaped gram-negative bacteria. *Mol Microbiol* 81:340–353.
17. Boulbitch A, Quinn B, Pink D (2000) Elasticity of the rod-shaped gram-negative eubacteria. *Phys Rev Lett* 85:5246–5249.
18. Deng Y, Sun M, Shaevitz JW (2011) Direct measurement of cell wall stress stiffening and turgor pressure in live bacterial cells. *Phys Rev Lett* 107:158101-1–158101-4.
19. Whatmore AM, Reeds RH (1990) Determination of turgor pressure in bacillus subtilis: a possible role for $k+$ in turgor regulation. *J Gen Microbiol* 136:2521–2526.
20. Peach M, Koehler JS (1950) The forces exerted on dislocations and the stress fields produced by them. *Phys Rev* 80:436–439.
21. Lamb H (1945) *Hydrodynamics* (Dover, New York).
22. Ispánovity PD, Groma I, Györgyi G, Szabó P, Hoffelner W (2011) Criticality of relaxation in dislocation systems. *Phys Rev Lett* 107:085506.
23. Ispánovity PD, Groma I, Györgyi G, Csikor FF, Weygand D (2010) Submicron plasticity: yield stress, dislocation avalanches, and velocity distribution. *Phys Rev Lett* 105:085503.
24. Angheluta L, Jeraldo P, Goldenfeld N (2012) arXiv:1201.5758.
25. Bruinsma R, Halperin BI, Zippelius A (1982) Motion of defects and stress relaxation in two-dimensional crystals. *Phys Rev B* 25:579–604.
26. Sliusarenko O, Cabeen MT, Wolgemuth CW, Jacobs-Wagner C, Emonet T (2010) Processivity of peptidoglycan synthesis provides a built-in mechanism for the robustness of straight-rod cell morphology. *Proc Natl Acad Sci USA* 107:10086–10091.
27. Takeuchi S, DiLuzio WR, Weibel DB, Whitesides GM (2005) Controlling the shape of filamentous cells of *Escherichia coli*. *Nano Lett* 5:1819–1823.
28. Wang P, et al. (2010) Robust growth of *Escherichia coli*. *Curr Biol* 20:1099–1103.
29. Cabeen MT, et al. (2009) Bacterial cell curvature through mechanical control of cell growth. *EMBO* 28:1208–1219.
30. Hagen SJ (2010) Exponential growth of bacteria: Constant multiplication through division. *Am J Phys* 78:1290–1296.
31. Scott M, Gunderson CW, Mateescu EM, Zhang Z, Hwa T (2010) Interdependence of cell growth and gene expression: Origins and consequences. *Science* 330:1099–1102.
32. Carmazine S, et al. (2003) *Self-Organization in Biological Systems* (Princeton University Press, Princeton).
33. Alon U (2006) *An Introduction to Systems Biology: Design Principles of Biological Circuits* (Chapman & Hall, London).
34. Camps O, Mahadevan L (2009) Shape and dynamics of tip-growing cells. *Curr Biol* 19:2102–2107.

Amir and Nelson